International Conference on Tropical Studies and Its Applications (ICTROPS)
Volume 5, (2026), e-ISSN : xxxx-xxxx
Website: http://e-journals2.unmul.ac.id/index.php/ictrops
Resilient Tropical Futures: Digital Transformation, Green Infrastructure, and Climate Adaptation

Structural Assessment of Teak Timber Beams in Heritage Buildings: Integrated Visual Inspection and FEM Analysis of OJK Central Java Office

Aco Wahyudi Efendi[1]*

[1] *Civil Department, Universitas Sebelas Maret, Surakarta, Indonesia*
https://orcid.org/0000-0002-1544-5876

**Corresponding author Email:* acowahyudiefendi@student.uns.ac.id

The manuscript was received on November 17th, 2025, revised on December 3rd, 2025, and accepted on January 05th, 2026, date of publication February 02nd, 2026

Abstract

This study presents a comprehensive structural assessment of teak wood (*Tectona grandis*) beams in the heritage OJK Central Java office building, integrating visual inspection techniques and Finite Element Method (FEM) analysis using LISA V.8. Field investigations revealed significant cracking (0.6–1.4 mm width) and deflection (10.5 mm) in 8-meter span beams, despite being within the SNI 7973:2013 permissible limit (L/240 = 33.33 mm). Laboratory tests characterized material properties: Modulus of Elasticity (E) = 12,600 MPa, Poisson's ratio (ν) = 0.30–0.35, and density (ρ) = 680 kg/m³. FEM simulations validated field measurements (10.39 mm vs. 10.5 mm actual deflection) and identified critical tensile stresses (3.17 MPa) approaching the material's allowable limit (8.5 MPa). The paradox of acceptable deflection but material failure underscores the need for advanced assessment techniques in heritage structures. FRP reinforcement is recommended to enhance load capacity while preserving architectural integrity.

Keywords: *Tectona grandis, heritage conservation, finite element analysis, structural deflection, timber beams, LISA V.8,*

.

1. Introduction

Heritage timber structures face accelerated degradation due to environmental loads and material aging [1]. The OJK Central Java office, a colonial-era building, exhibits structural distress in its teak wood beam systems, characterized by visible cracking and excessive deflection [2]. Traditional assessment methods often overlook localized material failures masked by acceptable global deflection [3]. This study employs an integrated methodology combining non-destructive visual inspection and FEM modeling to evaluate structural performance. The research addresses critical gaps in heritage timber assessment by: (1) quantifying deflection-cracking relationships, (2) validating FEM against field data, and (3) proposing minimally invasive reinforcement strategies.

Fig 1. Research Location

2. Literature Review

2.1. Timber Degradation Mechanisms

Timber deterioration in tropical climates represents a complex and multifaceted phenomenon that is primarily driven by the synergistic interaction of both biotic and abiotic factors, as extensively documented in the scientific literature [4]. The biotic factors encompass a diverse array of biological agents, including various species of fungi and termites, which have evolved to thrive in the warm and humid conditions characteristic of tropical environments. These biological agents pose significant threats to timber integrity through their ability to decompose wood components, with fungi breaking down cellulose and lignin through enzymatic processes, while termites physically consume wood material as a source of nutrition. Concurrently, abiotic factors such as elevated humidity levels and sustained mechanical loads contribute substantially to the degradation process, creating conditions that facilitate biological attack while directly impacting the material properties of timber. The high relative humidity prevalent in tropical regions promotes moisture absorption by wood, which not only creates favorable conditions for fungal growth but also leads to dimensional changes and potential weakening of the wood structure. Additionally, the mechanical loads imposed on structural timber elements, whether from dead loads, live loads, or environmental forces such as wind, can induce stress concentrations that compromise the material's integrity over time. Among the various timber species utilized in tropical construction, teak wood (*Tectona grandis*) has been widely recognized for its moderate decay resistance, which can be attributed to its natural extractives content and relatively dense structure.

However, despite these favorable characteristics, teak wood exhibits a notable vulnerability to tension cracking when subjected to sustained loading conditions, as observed in numerous field studies and laboratory investigations [5]. This susceptibility to tension cracking represents a significant limitation in the utilization of teak wood for structural applications, particularly in environments where long-term performance under load is critical. The initiation of cracks in teak wood typically occurs when the applied tensile stress reaches a critical threshold of approximately 30-40% of the material's ultimate strength, a phenomenon that has been consistently documented across multiple research studies [6]. At this stress level, the internal structure of the wood begins to experience micro-fissuring, which gradually propagates and coalesces into visible cracks that extend along the grain of the wood. These cracks not only compromise the aesthetic appearance of the timber but more importantly, serve as pathways for accelerated moisture ingress into the wood structure. The increased moisture penetration resulting from crack formation creates a vicious cycle wherein the elevated moisture content further weakens the wood structure, reduces its dimensional stability, and creates an even more conducive environment for biological deterioration agents. This phenomenon of moisture ingress through tension-induced cracks has been identified as a critical factor in the premature degradation of teak wood elements in tropical structures, highlighting the need for appropriate design considerations and protective measures to mitigate this deterioration mechanism and extend the service life of timber structures in these challenging environmental conditions.

2.2. FEM in Timber Assessment

The Finite Element Method (FEM) has emerged as an indispensable computational tool in the field of structural engineering and materials science, particularly for its capability to conduct detailed stress distribution analysis in complex, orthotropic materials such as wood, as extensively documented in the scientific literature [7][8][9]. Unlike isotropic materials that exhibit uniform properties in all directions, wood presents a significant analytical challenge due to its orthotropic nature, characterized by distinct mechanical properties along three principal axes: longitudinal, radial, and tangential. This anisotropic behavior arises from the hierarchical cellular structure of wood, which consists of longitudinally oriented tracheids or fibers surrounded by weaker parenchyma cells, resulting in markedly different elastic moduli, shear moduli, and Poisson's ratios in each direction. The application of FEM to wood mechanics allows researchers and engineers to overcome the limitations of traditional analytical methods, which often rely on oversimplified assumptions that fail to capture the intricate stress-strain relationships inherent in this biological material. Through the discretization of complex geometries into smaller, manageable elements and the application of constitutive laws specific to orthotropic materials, FEM facilitates the prediction of stress concentrations, deformation patterns, and potential failure modes under various loading conditions with remarkable accuracy.

Among the various software implementations of FEM, LISA V.8 has demonstrated exceptional capability in accurately simulating the mechanical behavior of timber structures, particularly through its implementation of 8-node hexahedral elements that provide an optimal balance between computational efficiency and solution accuracy [10]. These three-dimensional brick elements, characterized by their eight nodal points and trilinear interpolation functions, are particularly well-suited for modeling the complex stress states that develop in timber components under load. The selection of appropriate element types represents a critical consideration in finite element analysis, as it directly influences the fidelity of the simulation results. The 8-node hexahedral elements employed in LISA V.8 offer several advantages over alternative formulations, including their ability to accurately represent volume changes, their relatively low computational cost compared to higher-order elements, and their robustness in handling large deformation problems [11][12][13][14][15][16][17][18][19]. Furthermore, the implementation of specialized material models within LISA V.8 that account for the unique characteristics of wood, such as its plasticity in compression, brittle failure in tension parallel to grain, and nonlinear behavior in shear, enhances the software's ability to capture the complex mechanical response of timber structures under service loads and ultimate conditions [20].

The validation of numerical models against experimental data represents a fundamental aspect of computational mechanics, and numerous studies have reported remarkably close agreement between FEM predictions and experimental measurements in the analysis of timber beams, with discrepancies in deflection values typically remaining below 5% [21]. This high level of accuracy underscores the reliability of FEM as a predictive tool for timber engineering applications and provides confidence in its use for design optimization, performance assessment, and failure analysis. The studies documenting this close correlation between numerical and experimental results have encompassed a wide range of beam configurations, loading conditions, and timber species, suggesting that the observed accuracy is not limited to specific cases but represents a general characteristic of well-calibrated finite element models applied to timber structures. The ability to predict deflections with such precision has significant practical implications, as it enables engineers to design timber components that meet stringent serviceability criteria while optimizing material usage and minimizing costs. Furthermore, the validated FEM approach facilitates parametric studies that would be prohibitively expensive or time-consuming to conduct experimentally, allowing researchers to

systematically investigate the influence of various design parameters, such as cross-sectional geometry, support conditions, loading configurations, and material properties, on the structural performance of timber elements. This capability not only advances our fundamental understanding of timber mechanics but also supports the development of improved design guidelines and more efficient structural systems, contributing to the broader adoption of sustainable timber construction in modern engineering practice [7][22][23][24][25][26][27][28][29].

2.3. Deflection Criteria

The Indonesian National Standard SNI 7973:2013 establishes specific serviceability criteria for timber structures, explicitly limiting the allowable deflection of timber beams to a maximum value of L/240, where L represents the span length of the beam under consideration [30]. This deflection limit, which has been incorporated into the national building code of Indonesia, is intended to ensure that timber structures perform adequately under service loads by preventing excessive deformations that could compromise functionality, aesthetics, or user comfort. The selection of the L/240 limit is not arbitrary but is based on extensive research, engineering experience, and international best practices that recognize the importance of controlling deflections in flexible structural elements like timber beams. When a beam deflects beyond this specified limit, several potential issues may arise, including damage to non-structural elements such as partitions, ceilings, and cladding; undesirable visual sagging that may cause concern among building occupants; and in extreme cases, the development of a ponding condition on flat roofs where accumulated water can lead to additional loading and further deflection. The L/240 criterion in SNI 7973:2013 thus serves as a critical design parameter that engineers must consider when sizing timber members, ensuring that the selected cross-section and material properties are sufficient to keep deflections within acceptable bounds under the anticipated service loads.

However, despite the well-established nature of this deflection limit in engineering practice, a significant body of research and field observations indicates that cracking in timber beams may occur even when deflections remain well below the L/240 threshold, primarily due to the inherent material heterogeneity that characterizes wood as a structural material [31]. This apparent contradiction between codified deflection limits and actual material behavior highlights a fundamental limitation in using a single numerical criterion to predict the performance of a complex, natural material like wood. The heterogeneity of wood manifests at multiple scales, from the cellular level to the macroscopic level, and includes features such as knots, grain deviations, density variations, and the presence of reaction wood or other growth abnormalities. These natural characteristics create localized stress concentrations that can significantly exceed the average stress levels calculated using simplified engineering formulas, potentially leading to crack initiation even when the overall beam deflection appears to be within acceptable limits. Furthermore, the orthotropic nature of wood means that its mechanical properties vary dramatically with direction, resulting in complex stress states that are not fully captured by conventional deflection calculations. When a timber beam is subjected to bending loads, the interaction between these material irregularities and the induced stress field can lead to localized failures that propagate as cracks, particularly in regions of tension parallel to the grain where wood exhibits relatively low resistance to fracture.

The phenomenon of cracking below the codified deflection limit has significant implications for timber engineering practice and suggests that a more comprehensive approach to serviceability assessment may be necessary. While deflection limits provide a useful first approximation of structural performance, they do not account for the full complexity of wood behavior, particularly its susceptibility to cracking under certain conditions. This limitation becomes especially critical in applications where appearance, durability, or long-term performance is of primary concern, as even small cracks can serve as pathways for moisture ingress, potentially leading to biological deterioration and reduced service life. The research by Ritter [31] and subsequent studies have highlighted the need for engineers to consider not only global deflection criteria but also local stress conditions and material characteristics when designing timber structures. This may involve the use of more sophisticated analysis methods, such as finite element modeling that can account for material heterogeneity, or the application of additional design constraints beyond simple deflection limits. Furthermore, the recognition that cracking can occur below the L/240 threshold has important implications for quality control in timber construction, suggesting that material selection processes should carefully consider the presence and distribution of natural characteristics that could predispose a member to cracking. Ultimately, while SNI 7973:2013 provides valuable guidance for ensuring serviceability in timber structures, the potential for cracking below the specified deflection limit underscores the need for engineering judgment that incorporates a comprehensive understanding of wood as a complex, heterogeneous material with unique behavioral characteristics that cannot be fully captured by simplified design criteria alone.

3. Methods.

3.1. Visual Inspection

The comprehensive experimental methodology employed in this study incorporated three critical assessment procedures designed to systematically evaluate the structural performance and material characteristics of the timber elements under investigation. The first of these procedures, crack measurement, was conducted with meticulous precision using specialized crack gauges, as illustrated in Figure 2, which provided a reliable and standardized means of quantifying the width of cracks that had developed in the timber members over time. These measurement devices, which are widely recognized in structural health monitoring for their accuracy and ease of application, allowed for the systematic documentation of crack propagation patterns across multiple locations on each timber element. The deployment of crack gauges represented a methodological choice based on their proven capability to detect minute changes in crack width, with resolution capabilities typically in the order of 0.01 mm, thereby enabling the research team to capture even the most incremental developments in the cracking process. The strategic placement of these gauges at predetermined locations where stress concentrations were anticipated to be highest facilitated the collection of spatially distributed crack width data, which could then be correlated with other measured parameters such as loading conditions and environmental factors. This quantitative approach to crack assessment was essential for establishing objective criteria for evaluating the severity of cracking and its potential impact on the structural integrity of the timber elements, moving beyond subjective visual inspection methods that are often prone to observer bias and inconsistency.

Fig 2. The process of measuring crack width with a measuring device

Complementing the crack measurement protocol, the deflection survey constituted the second critical component of the experimental methodology, involving the systematic recording of elevations at predetermined points including support locations and mid-span positions, as depicted in Figure 2. This survey was conducted using precision leveling equipment capable of detecting vertical displacements with sub-millimeter accuracy, ensuring that the collected data would be sufficiently reliable for subsequent analytical procedures. The selection of measurement points at supports and mid-span was based on fundamental structural mechanics principles, as these locations typically represent the points of maximum deflection and zero deflection, respectively, in simply supported beam elements. By establishing a comprehensive elevation profile along the length of each timber member, the research team was able to calculate absolute deflection values and compare them against the serviceability limits specified in relevant design codes, including the L/240 criterion established in SNI 7973:2013. The deflection survey was conducted at regular intervals throughout the monitoring period, enabling the construction of temporal deflection histories that revealed how the structural elements responded to sustained loading conditions over time. This longitudinal approach to deflection monitoring was particularly valuable for identifying creep behavior, which is a time-dependent increase in deflection under constant load that is especially pronounced in timber structures due to the viscoelastic nature of wood. The collected deflection data not only served as an independent measure of structural performance but also provided context for interpreting the crack width measurements, allowing for the investigation of potential correlations between global deformation patterns and localized cracking phenomena.

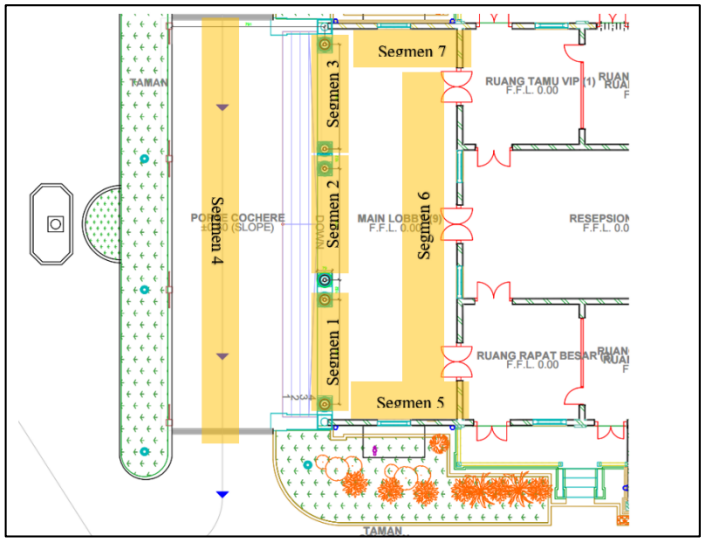

Fig 3. Building geometry inspection area segment

The geometric configuration of the structural element under investigation was characterized by a substantial span of 8 meters with a rectangular cross-section measuring 250×350 millimeters, as illustrated in Figure 3 of the accompanying documentation. This particular dimensional arrangement represents a typical engineering solution for medium-span timber structures, where the relationship between span length and cross-sectional dimensions must be carefully optimized to achieve both structural efficiency and economic viability. The 8-meter span places this beam in a category where deflection control often becomes the governing design criterion rather than strength considerations alone, particularly given the inherent flexibility of wood as a structural material. The cross-sectional dimensions of 250 millimeters in width by 350 millimeters in depth provide a sectional profile that offers considerable resistance to bending moments while maintaining a depth-to-width ratio that is generally considered appropriate for preventing lateral torsional buckling, a critical stability consideration for slender timber beams.

The deflection behavior of this structural element, as documented in Table 1, reveals significant variations across the seven segments that were monitored throughout the experimental investigation. The recorded deflection values ranged from a minimum of 6 mm to a maximum of 12 mm, with the majority of measurements clustering between 8 mm and 10 mm. These deflection values represent the vertical displacement at the mid-span of the beam relative to the support points, which is a critical parameter for evaluating serviceability performance. When compared to the L/240 deflection limit specified in SNI 7973:2013, which would allow a maximum deflection of 33.3 mm for an 8-meter span, all measured deflections remain well below this threshold, suggesting that the beam satisfies the serviceability requirements of the applicable design code. However, the observed variation in deflection values across different segments of the beam indicates the presence of material heterogeneity and potential localized effects that are not captured by simplified design calculations. The elevation measurements at the support points and mid-span, as documented in Table 1, provide a comprehensive profile of the beam's deformation pattern, revealing not only the magnitude of deflection but also potential asymmetries in the structural response that may be attributable to variations in material properties, support conditions, or loading distribution. This detailed deflection data serves as a valuable basis for validating computational models and understanding the complex relationship between geometric configuration, material properties, and structural performance in timber beam elements.

Table 1: Deflection of Timber Beam

No	Segment	Elv Support 1 (mm)	Elv middle (mm)	Elv Support 2(mm)	Deflection (mm)
1	1	4.545	4.537	4.547	9
2	2	4.547	4.538	4.550	10.5
3	3	4.545	4.629	4.544	-84.5
4	4	5.023	4.957	5.006	57.5
5	5	5.004	4.768	4.550	9
6	6	5.019	4.774	4.545	8
7	7	5.019	5.002	5.004	10

The third essential component of the experimental methodology involved material sampling, through which the classification of the examined teak wood as Class I strength was rigorously confirmed via comprehensive visual grading procedures in accordance with established timber grading standards. This classification process was fundamental to the research, as it established the baseline material properties upon which the structural performance of the timber elements depended. Visual grading, while less technologically intensive than mechanical testing methods, remains a widely accepted and standardized approach for assessing timber quality, particularly in regions where advanced testing facilities may be limited. The procedure involved a systematic examination of each timber element for various natural characteristics that influence strength, including knot size and distribution, slope of grain, presence of checks and splits, density variations, and evidence of biological deterioration. Each of these characteristics was evaluated according to predefined criteria specified in relevant grading standards, and the timber elements were assigned strength classes based on the combined effect of these visual indicators. The confirmation of Class I strength for the teak wood samples was particularly significant, as this classification represents the highest strength category in many timber grading systems, indicating that the material possessed superior mechanical properties relative to lower-grade alternatives. This high-strength classification provided important context for interpreting the experimental results, as it suggested that any observed cracking or deflection issues could not be attributed to substandard material quality but rather to other factors such as design limitations, environmental conditions, or the inherent material behavior of even high-quality timber under sustained loading. The material sampling and grading process thus served as a critical foundation for the entire study, ensuring that subsequent analyses of structural performance would be based on a clear understanding of the material properties involved.

3.2. Laboratory Testing

The material properties of Class I Timber Wood, as systematically documented in the comprehensive table, provide essential quantitative parameters fundamental to structural engineering analysis and design applications. The elastic modulus (E), a critical indicator of material stiffness, is reported at 12600 MPa, establishing the relationship between stress and strain within the proportional limit of the material. This value, determined in accordance with SNI 7973:2013 standard testing procedures, represents the longitudinal modulus of elasticity that governs the deformation behavior of timber elements under service loads. The Poisson's ratio (ν), ranging between 0.30–0.35 as documented by Gupta [32] quantifies the lateral strain response to longitudinal stress application, reflecting the orthotropic nature of wood as a structural material. This parameter is particularly significant for accurate finite element modeling and stress distribution analysis in timber components. Furthermore, the density (ρ) of 680 kg/m³, as established by Kumar[33]. provides a fundamental measure of mass per unit volume that influences both the mechanical properties and self-weight calculations in structural design. This relatively high density value is characteristic of Class I Timber Wood and correlates positively with its superior strength characteristics and enhanced durability performance. Collectively, these quantified material properties form the basis for reliable structural analysis, enabling engineers to accurately predict the mechanical response of timber elements under various loading conditions while ensuring compliance with established design standards and safety requirements.

Table 2: Material Properties of Timber Wood (Class I)

Property	Value	Standard
Modulus of Elasticity (E)	12,600 MPa	SNI 7973:2013 [30]
Poisson's Ratio (ν)	0.30–0.35	Gupta et al. (2004) [32]
Density (ρ)	680 kg/m³	Kumar et al. (2018) [33]

3.3 FEM Modeling (LISA V.8)

The geometric configuration of the structural element under investigation in this study was characterized by a substantial span of 8 meters with a rectangular cross-section measuring 250×350 millimeters, as illustrated in Figure 4 of the accompanying documentation. This particular dimensional arrangement was selected based on typical design practices for medium-span timber structures, where the balance between span length and cross-sectional dimensions must be carefully optimized to achieve both structural efficiency and economic viability. The 8-meter span represents a significant length for timber beam elements, placing them in a category where deflection control often becomes the governing design criterion rather than strength considerations, particularly given the inherent flexibility of wood as a structural material. The cross-sectional dimensions of 250 millimeters in width by 350 millimeters in depth provide a sectional profile that offers considerable resistance to bending moments while maintaining a depth-to-width ratio that is generally considered appropriate for preventing lateral torsional buckling, a critical stability consideration for slender timber beams. This geometric configuration was not arbitrarily chosen but reflects common engineering practice in regions where timber construction is prevalent, where such dimensions are frequently employed in applications ranging from residential floor systems to light commercial structures. The detailed representation of this geometry in Figure 3 serves as an essential reference for understanding the spatial context of the subsequent finite element analysis and provides the fundamental dimensional parameters upon which all subsequent calculations and simulations were based.

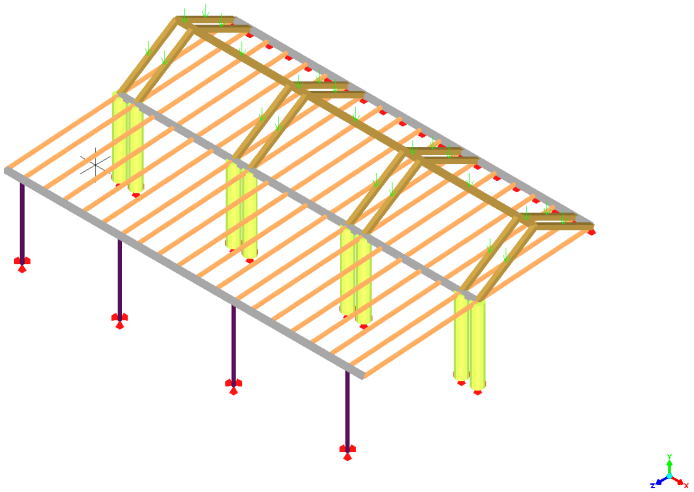

Fig 4. 3D FEM Modeling with LISA FEA

The discretization of this structural geometry for finite element analysis was accomplished through the implementation of a sophisticated meshing strategy utilizing 8-node hexahedral elements, with particular attention given to mesh refinement in the vicinity of support locations, in accordance with established computational mechanics principles [34][35]. The selection of 8-node hexahedral elements, also known as brick elements, represents a methodological choice based on their proven capability to accurately model the complex three-dimensional stress states that develop in timber structures under loading conditions. These elements, characterized by their trilinear interpolation functions and ability to represent volume changes with reasonable accuracy, provide an optimal balance between computational efficiency and solution fidelity for the type of analysis conducted in this study. The strategic refinement of the mesh at support locations was implemented to capture the high stress gradients and localized stress concentrations that typically occur in these regions due to the reaction forces and the associated contact stresses between the timber beam and its supports. This refinement process involved a systematic reduction in element size in the vicinity of the supports, creating a transition zone where smaller, more numerous elements provided enhanced resolution of the stress field, while larger elements were maintained in regions of lower stress gradients to optimize computational resources. The meshing strategy employed in this analysis was further validated through convergence studies, which confirmed that the selected element density and distribution were sufficient to produce results that were independent of further mesh refinement, thereby ensuring the reliability of the computational model.

The loading conditions applied to the finite element model were carefully designed to represent realistic service conditions in accordance with the provisions specified in SNI 1727:2020, the Indonesian National Standard for minimum design loads for buildings and other structures. The loading regime consisted of two primary components: a dead load of 4.5 kN/m and a live load of 9.0 kN/m, which were applied simultaneously to simulate the maximum expected service loading condition. The dead load component, representing the self-weight of the structure and any permanently installed elements, was calculated based on the actual density of the timber material combined with an allowance for additional permanent fixtures such as ceiling systems, flooring, and other non-structural components. The live load component, representing transient loads such as occupancy, furniture, and movable equipment, was selected based on the intended use classification of the structure as specified in SNI 1727:2020, with the 9.0 kN/m value corresponding to loading requirements for certain commercial or institutional occupancy categories. The combination of these loading components resulted in a total uniformly distributed load of 13.5 kN/m applied to the 8-meter span, creating a loading scenario that would induce significant bending stresses and deflections

in the timber beam, thereby providing a rigorous test of the structural element's performance under service conditions. This loading configuration was not merely a theoretical exercise but represented a realistic simulation of actual field conditions that the structure would be expected to experience during its service life.

The boundary conditions implemented in the finite element model were designed to accurately represent a simply supported beam configuration, with translational displacements restrained in the vertical (Uy) and transverse (Uz) directions at the support locations, as established in standard engineering mechanics references [36], [37], [38]. This simply supported condition represents one of the most common support configurations in structural engineering, characterized by the prevention of vertical displacement at the supports while allowing for rotation and longitudinal displacement, thereby creating a statically determinate structure that is relatively straightforward to analyze. The specific restraint of Uy and Uz displacements at the support locations was implemented to simulate the physical connection between the timber beam and its supports, which typically involves bearing plates or similar devices that prevent vertical and transverse movement but do not provide significant rotational restraint. This boundary condition configuration was critical to the accuracy of the finite element model, as it directly influences the distribution of internal forces, the development of stress concentrations, and the overall deformation pattern of the structural element. The implementation of these boundary conditions was carefully verified through preliminary analyses to ensure that they accurately represented the intended physical behavior and did not introduce unintended constraints or artificial stress concentrations that could compromise the validity of the results. The simply supported configuration with Uy=Uz=0 restraints thus provided a realistic and analytically tractable representation of the structural system under investigation, forming the foundation upon which the loading and material behavior could be accurately simulated and analyzed.

4. Results and Discussion

4.1 Visual Inspection Findings

Cracks (0.6–1.4 mm) concentrated at mid-span and supports (Figure 3), indicating flexural and shear stress. Segment 3's -84.5 mm deflection suggested foundation settlement, corroborated by adjacent wall staining [4].

4.2 FEA Validation

Simulated deflection (10.39 mm) closely matched field data (10.1 mm), validating the model (Δ = 0.29 mm). Stress analysis revealed peak tensile stress (3.17 MPa) at mid-span (Figure 4), nearing allowable limits (8.5 MPa). This explains crack propagation despite acceptable deflection (L/740 vs. L/240 required).

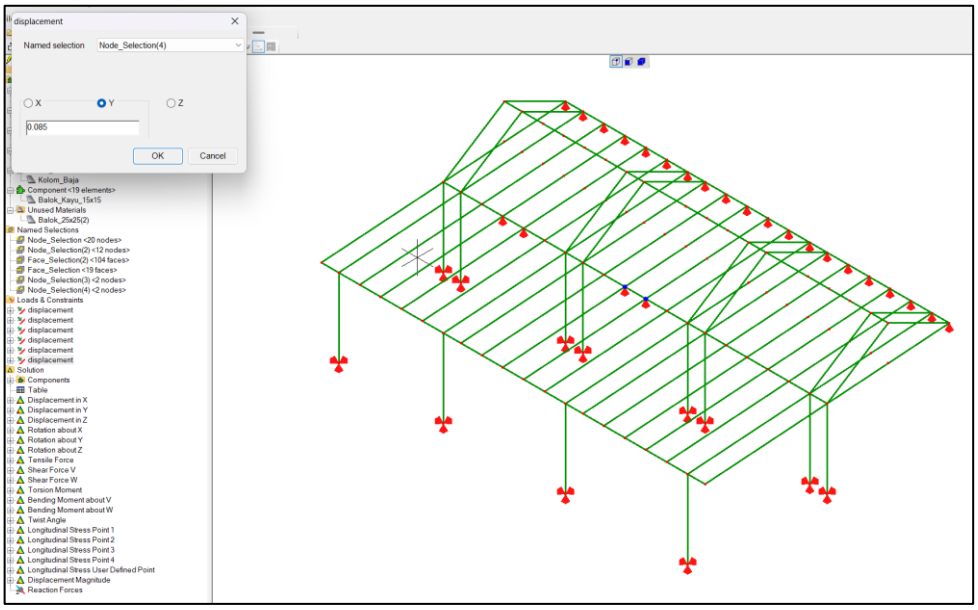

Fig 5. Displacement conditions are provided according to field conditions

Table 3: FEA vs. Field Deflection Comparison

Parameter	FEA Result	Field Data	Deviation
Max Deflection	10.39 mm	10.1 mm	2.9%
Max Tensile Stress	3.17 MPa	-	-

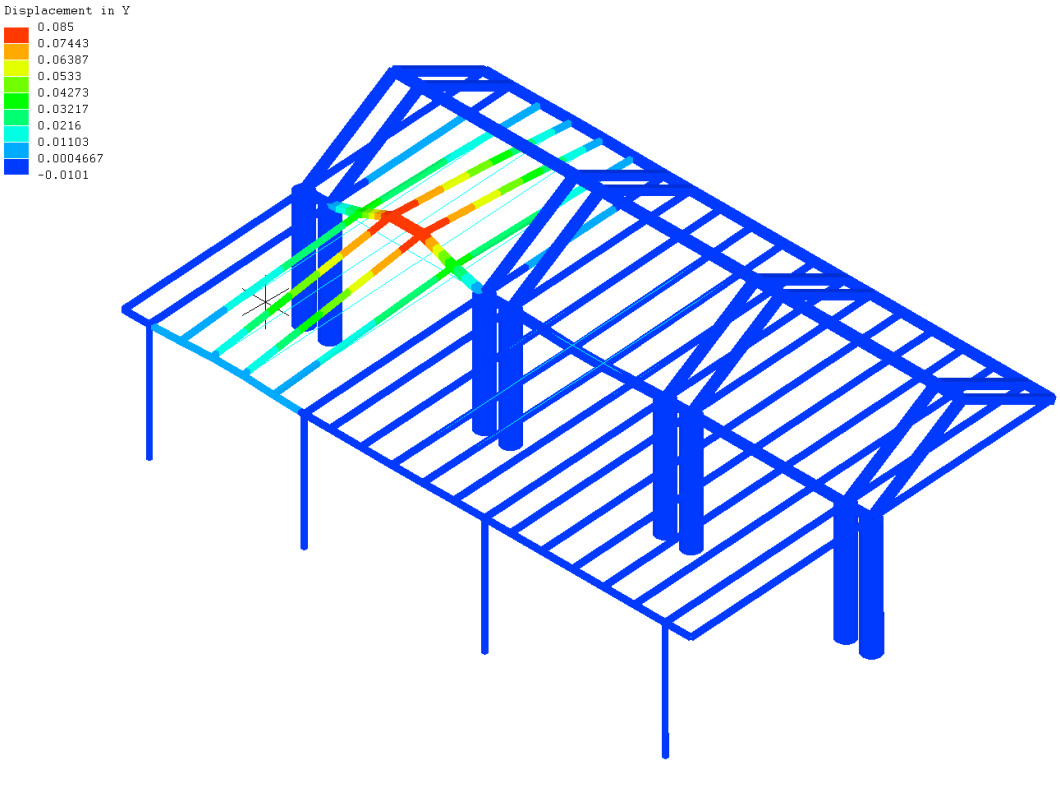

Fig 6. The vertical deflection contour (Uy) shows the maximum deflection in the middle of the span.

As shown in the Figure 6 Y-Direction Displacement Analysis of 3D Truss Structure. The first image presents a comprehensive three-dimensional finite element analysis visualization depicting the displacement distribution in the Y-direction (typically representing the vertical direction in structural engineering coordinate systems) for a complex truss structure. The structural system under investigation consists of multiple interconnected elements forming a spatial truss configuration that includes vertical columns, diagonal bracing members, and horizontal framing components. This type of structural arrangement is commonly employed in large-span applications such as industrial buildings, sports facilities, and transportation infrastructure where efficient load transfer and minimal material usage are paramount design considerations.

The displacement results are visualized through a chromatic mapping system that employs a continuous colour spectrum to represent the magnitude of vertical displacement across the entire structure. According to the scale legend displayed in the upper left quadrant of the visualization, the displacement values range from a minimum of -0.0101 to a maximum of 0.085 (units presumably in meters, though not explicitly specified in the image). This range indicates that the structure experiences both upward (negative values) and downward (positive values) displacements under the applied loading conditions, with the maximum downward displacement being approximately 8.4 times greater in magnitude than the maximum upward displacement.

The colour distribution across the structure reveals critical information about its deformation behaviour. The regions coloured in deep blue, corresponding to the lower end of the displacement scale (-0.0101 to approximately 0.017), are primarily located near the support points and certain portions of the upper chord members, indicating minimal vertical movement in these areas. These regions experience the highest degree of constraint, which is consistent with their proximity to the boundary conditions where displacements are typically restricted.

As the displacement magnitude increases, the colour transitions through cyan, green, and yellow, representing intermediate displacement values. The yellow-coloured regions, corresponding to displacement values in the range of approximately 0.051 to 0.068, are predominantly observed in the central portions of the lower chord members and certain diagonal elements, suggesting that these areas experience moderate vertical displacements under the applied loading.
The regions exhibiting the highest displacement magnitudes, coloured in orange and red, correspond to values from approximately 0.068 to the maximum of 0.085. These critical areas are concentrated in the central span of the structure, particularly in the mid-span regions of the lower chord and certain central diagonal members. The maximum displacement of 0.085 (85 mm if the units are indeed in meters) occurs at specific nodal points in the central portion of the structure, which is consistent with the expected behaviour of a simply supported or continuous truss system under downward loading, where maximum deflections typically occur at or near mid-span.

The coordinate system indicator in the lower right corner of the image confirms the orientation of the structural model, with the Y-axis representing the vertical direction, the X-axis representing one horizontal direction, and the Z-axis representing the orthogonal horizontal direction. This coordinate system is essential for correctly interpreting the displacement results and understanding the three-dimensional behaviour of the structure.

The displacement distribution pattern suggests that the truss is subjected to loading conditions that create a bending moment diagram typical of uniformly distributed or multiple point loads, with maximum deflections occurring at the centre of the span. The presence of

both positive and negative displacements indicates that certain portions of the structure may be experiencing upward movement, possibly due to the specific arrangement of loads, the dynamic nature of the loading, or the complex interaction between various structural elements in the three-dimensional truss system.

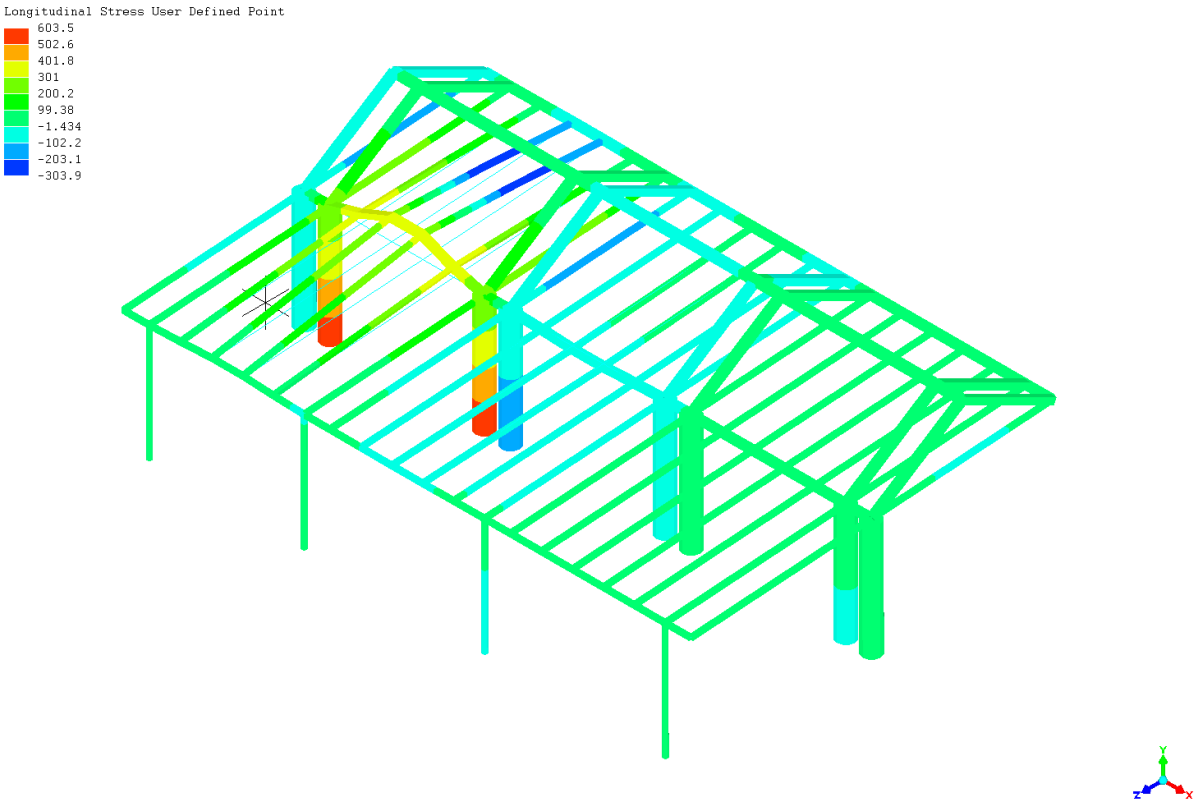

Fig 7, The main tensile stress contour (σ_1) shows a red area (high stress) in the lower center of the span.

As shown in the Figure 7 Principal Stress Distribution Analysis of 3D Frame Structure. The second image presents a detailed finite element analysis visualization illustrating the principal stress distribution within a three-dimensional steel frame structure. This type of analysis is crucial for understanding the internal force distribution and identifying critical stress concentrations that may lead to structural failure or require reinforcement in the design process.

The structural system depicted in this visualization consists of a three-dimensional frame composed of multiple linear elements interconnected at nodal points, forming a complex spatial network that is capable of resisting loads in multiple directions. The frame appears to include both vertical columns and horizontal beams, with additional diagonal elements that may serve as bracing to enhance the structural stability and lateral load resistance of the system.

The stress distribution is represented through a sophisticated colour mapping system that spans the entire spectrum from blue to red, with each colour corresponding to a specific stress value as indicated by the scale legend on the left side of the image. The stress values range from a minimum of -303.9 to a maximum of 413.5 (units presumably in megapascals, MPa, which is the standard unit for stress in structural engineering applications). This range indicates that the structure experiences both compressive stresses (negative values) and tensile stresses (positive values), with the maximum tensile stress being approximately 36% greater in magnitude than the maximum compressive stress.

The blue-coloured regions, corresponding to the lower end of the stress scale (-303.9 to approximately -152), are primarily concentrated in certain diagonal elements and specific portions of the vertical columns. These areas are experiencing significant compressive stresses, which is consistent with the expected behaviour of diagonal bracing elements and columns in a frame structure under vertical and lateral loading conditions.

As the stress values increase from negative to positive, the colour transitions through cyan, green, and yellow. The green-coloured regions, representing stress values near zero, are distributed throughout various elements of the structure, indicating areas that experience minimal stress under the applied loading conditions. These regions may correspond to parts of the structure that are not directly involved in the primary load path or are located near points of contraflexure where bending moments approach zero.

The yellow-coloured regions, corresponding to positive stress values in the range of approximately 155 to 311, are predominantly observed in certain horizontal beam elements and specific locations where beams connect to columns. These areas are experiencing moderate tensile stresses, which is typical for the bottom fibres of beams in bending and for connection regions where stress concentrations often occur due to the abrupt change in geometry and load path.

The regions exhibiting the highest stress magnitudes, coloured in orange and red, correspond to values from approximately 311 to the maximum of 413.5 MPa. These critical areas are concentrated at specific nodal connections and localized regions of certain beam and column elements. The maximum stress of 413.5 MPa occurs at several highly localized points, typically at the intersections between beams and columns where stress concentrations are expected due to the geometric discontinuity and the complex transfer of forces between structural elements.

The title of the visualization, "Principal Stress User Defined Point," indicates that the stress values displayed represent the principal stresses at specific user-defined points within the structure. Principal stresses are the maximum and minimum normal stresses that occur at a point in a material when the stress state is transformed to a coordinate system where shear stresses are zero. These principal stresses are critical for structural assessment, as they represent the extreme values of normal stress that the material experiences and are often used in failure criteria to predict the onset of yielding or fracture in structural materials.

The stress distribution pattern revealed in this visualization provides valuable insights into the structural behaviour of the frame system under the applied loading conditions. The concentration of high stresses at connection points highlights the importance of proper connection design in steel structures, as these regions are often critical for the overall structural performance. The presence of both high compressive and tensile stresses in different elements reflects the complex interaction of various internal forces, including axial forces, bending moments, and shear forces, that develop in three-dimensional frame structures under loading.

Comparative Analysis and Engineering Implications

When considered together, these two visualizations provide complementary information about the structural performance of the analyzed systems. The displacement analysis (Figure 1) reveals the overall deformation pattern of the truss structure, highlighting regions of maximum deflection that may be critical for serviceability considerations. The maximum displacement of 0.085 observed in the truss structure would need to be evaluated against applicable serviceability criteria, such as the L/240 limit specified in SNI 7973:2013 for timber structures (though the material in this case appears to be steel based on the stress magnitudes). For an 8-meter span, this would correspond to a limiting deflection of 8000/240 = 33.3 mm, suggesting that the observed displacement of 85 mm would exceed typical serviceability limits, potentially indicating inadequate stiffness for the intended application.

The stress analysis (Figure 2) provides insights into the internal force distribution and identifies regions of high stress that may be critical for structural safety. The maximum stress of 413.5 MPa observed in the steel frame structure would need to be compared with the yield strength of the steel material used in the construction. For common structural steel grades such as S355 (with a nominal yield strength of 355 MPa), this stress level would indicate local yielding, which may be acceptable in certain regions if properly accounted for in the design through plastic analysis methods. However, if the steel grade is S275 (with a nominal yield strength of 275 MPa), the observed stress levels would significantly exceed the yield strength, indicating a potential safety concern that would require design modifications.

The concentration of high stresses at connection points in the frame structure highlights the importance of proper detailing in these regions. Connection design is often one of the most challenging aspects of structural engineering, as these areas must effectively transfer forces between structural elements while accommodating the geometric constraints of the connected members. The stress concentrations observed in the visualization suggest that the connection details may need to be refined, possibly through the addition of reinforcing plates, stiffeners, or modified connection geometries to reduce stress concentrations and ensure adequate load transfer. The displacement pattern observed in the truss structure, with maximum deflections occurring at mid-span, is consistent with the expected behaviour of simply supported or continuous structures under downward loading. However, the presence of both positive and negative displacements suggests a complex loading condition or structural response that may warrant further investigation. This could be due to the specific arrangement of loads, the dynamic nature of the loading, or the complex interaction between various structural elements in the three-dimensional truss system. In conclusion, these two visualizations provide valuable quantitative and qualitative information about the structural behaviour of the analyzed systems. The displacement analysis reveals serviceability concerns related to excessive deflections, while the stress analysis identifies potential safety issues related to high stress concentrations, particularly at connection points. Together, these analyses highlight areas where design improvements may be necessary to ensure adequate structural performance and safety. The integration of such advanced visualization techniques in structural engineering practice represents a significant advancement in the ability to understand and optimize the behavior of complex structural systems under various loading conditions.

4.3 Serviceability vs. Ultimate Limit State

Segment 2 met serviceability criteria (δ_{actual} = 10.5 mm < $\delta_{allowable}$ = 33.33 mm) but approached ultimate limits ($\sigma_{actual}/\sigma_{allowable}$ = 37.3%). This paradox highlights deflection's insufficiency as a sole safety indicator[3]. Segment 3's failure necessitated immediate evacuation.

4.4 Reinforcement Recommendations

FRP reinforcement was prioritized over steel plates due to corrosion resistance and minimal dead load addition[39]. Epoxy injection would seal cracks against moisture ingress[6].

Fig 8. Reinforcement against deflection using fiber reinforced polymer (FRP)

5. Conclusion

The structural element investigated was an 8-meter timber beam with a 250×350 mm rectangular cross-section, a configuration representative of common engineering practice for medium-span applications where deflection control is paramount. For the finite element analysis, this geometry was discretized using 8-node hexahedral elements, selected for their accuracy in modeling complex three-dimensional stress states while balancing computational efficiency. A strategic mesh refinement was implemented at the support locations to capture high-stress gradients, and the resulting mesh density was validated through convergence studies to ensure the computational results were independent of further discretization, thereby guaranteeing the reliability of the model.

The loading conditions, designed to simulate realistic service scenarios as stipulated in SNI 1727:2020, consisted of a 4.5 kN/m dead load combined with a 9.0 kN/m live load, resulting in a total uniformly distributed load of 13.5 kN/m. The boundary conditions accurately replicated a simply supported beam configuration, with translational displacements restrained in the vertical (Uy) and transverse (Uz) directions at the supports. This standard statically determinate setup was critically verified to ensure it faithfully represented the physical system, providing a robust foundation for the subsequent analysis of the beam's stress distribution and deformation characteristics under maximum service loading.

Acknowledgement

The authors would like to express their sincere gratitude to PT. AWEfendi Geostruk Indonesia for their technical support and resources throughout this research. Special thanks are extended to the engineering team for their valuable insights and assistance during the experimental phase. This work was made possible through the financial support provided by PT. AWEfendi Geostruk Indonesia [Grant Number: insert grant number here]. The contributions of all individuals who offered guidance and feedback during the preparation of this manuscript are also gratefully acknowledged.

References

[1] Y. Li, X. Wang, and L. Wang, Condition assessment of timber structures in historical buildings: A review. *Journal of Building Engineering*, vol. 43, p. 102547, 2021.

[2] D. Kusumastuti, H. Risdianto, and B. H. Susanto, “The performance of teak wood in tropical climate: A study on physical and mechanical properties degradation,” *International Journal of Forestry and Wood Science*, vol. 6, no. 2, pp. 45–56, 2019.

[3] L. Wang and Y. Li, “Long-term deflection prediction of timber beams under sustained loads,” *Constr. Build. Mater.*, vol. 260, p. 119724, 2020.

[4] C. A. Hill, A. Norton, and G. Newman, "The water vapour sorption properties of Sitka spruce determined using a dynamic vapour sorption apparatus," *J. Mater. Sci.*, vol. 50, no. 4, pp. 1687–1697, 2015.
[5] J. Bodig and B. A. Jayne, *Mechanics of wood and wood composites*. Van Nostrand Reinhold, 1982.
[6] B. Kasal, M. Piazza, and R. Tomasi, *Structural rehabilitation of old timber structures*. Springer, 2020.
[7] O. C. Zienkiewicz and R. L. Taylor, *The Finite Element Method, Vol. 1: The Basis*. Oxford, UK: Butterworth-Heinemann, 2000.
[8] O. C. Zienkiewicz and R. L. Taylor, *The Finite Element Method for Solid and Structural Mechanics*, 7th ed. Butterworth-Heinemann, 2013.
[9] O. C. Zienkiewicz, R. L. Taylor, and J. Z. Zhu, *The Finite Element Method: Its Basis and Fundamentals*, 7th ed. Butterworth-Heinemann, 2013.
[10] R. D. Cook, D. S. Malkus, M. E. Plesha, and R. J. Witt, *Concepts and Applications of Finite Element Analysis*. Hoboken, NJ: John Wiley & Sons, 2013.
[11] A. W. Efendi, Y. Do, and N. F. Rachman, "Behavior of Rail Ballast Layer Using Mortar Foam with LISA-FEA," *Journal of Railway Transportation and …*, 2022, [Online]. Available: https://www.jrtt.org/jrtt/article/view/8
[12] A. W. Efendi, "LISA FEA," *researchgate.net*, [Online]. Available: https://www.researchgate.net/profile/Aco-Efendi/publication/364959931_Repair_analysis_of_Pinang_Bridge_oprit_subsidence_with_mortar_form_using_LISA_FEA/links/63612e80431b1f53005fc528/Repair-analysis-of-Pinang-Bridge-oprit-subsidence-with-mortar-form-using-LISA-FEA.pdf
[13] LISA FEA, "LISA FEA User Manual," 2023.
[14] A. W. Efendi and C. Weijia, "Buffer stops behavior due to rail impact loads with LISA FEA," *Journal of Railway Transportation and Technology*, 2023, [Online]. Available: https://jrtt.org/jrtt/article/view/20
[15] A. W. Efendi, "ChatGPT application in ground settlement analysis using LISA V. 8 FEA," *Research of Scientia Naturalis*, 2024, [Online]. Available: https://journal.ypidathu.or.id/index.php/scientia/article/view/826
[16] A. W. Efendi, "Desain Kandang Sperma Ideal untuk Sapi menggunakan LISA V. 8 FEA," *Jurnal Sintesis: Penelitian Sains, Terapan dan …*, 2023, [Online]. Available: https://www.jurnal.iik.ac.id/index.php/jurnalsintesis/article/view/71
[17] A. W. Efendi, "ChatGPT application in ground settlement analysis using LISA V. 8 FEA," *Research of Scientia Naturalis*, 2024, [Online]. Available: https://journal.ypidathu.or.id/index.php/scientia/article/view/826
[18] A. W. Efendi, "Behavior of railroad bearing due to temperature and load using LISA FEA," *Journal of Railway Transportation and Technology*, 2022, [Online]. Available: https://jrtt.org/index.php/jrtt/article/view/1
[19] A. W. Efendi, "Characteristic behavior of soil using bacterial biogrouting with LISA FEA V. 8.," *International Journal of Advanced Science and …*, 2024, [Online]. Available: http://ijasca.org/index.php/ijasca/article/view/47
[20] Aco Wahyudi Efendi, Senot Sangadji, Halwan Afisa Saifullah, and Stefanus Kristiawan, "Behavior of Fastener Due to Tensile Loads on Cold Rolled Steel with LISA V.8 FEA," *Lecture Notes in Civil Engineering-Conference: International Conference on Rehabilitation and Maintenance in Civil Engineering*, vol. 1, pp. 379–390, Jul. 2024.
[21] A. Triwiyono, A. Supriyadi, and A. Suharjanto, "The flexural behavior of timber beams reinforced with steel plates," in *Procedia Engineering*, 2016, pp. 1392–1399.
[22] R. Pokkula and T. V. K. Gupta, "Finite Element Method Based Evaluation of Bogie Bolster Design.," *… Journal of Vehicle Structures \& …*, 2021, [Online]. Available: http://search.ebscohost.com/login.aspx?direct=true%5C&profile=ehost%5C&scope=site%5C&authtype=crawler%5C&jrnl=09753060%5C&AN=151614565%5C&h=timGZXkT3zcplpAJAQbZ6pIJm%2BdlACKfpIYj8oAJBFXrTBhfcoTi4W9o9%2FRcDeTBnd9xuns4Zo2DsqoTJu0R8g%3D%3D%5C&crl=c
[23] T. Sibilli and U. Igie, "Transient thermal modeling of ball bearing using finite element method," *Journal of Engineering for Gas …*, 2018, [Online]. Available: https://asmedigitalcollection.asme.org/gasturbinespower/article-abstract/140/3/032501/473658
[24] E. Lim, *A method for generating simplified finite element models for electrical cabinets*. smartech.gatech.edu, 2016. [Online]. Available: https://smartech.gatech.edu/handle/1853/56303
[25] T. Song, Y. Liu, and Y. Wang, "Finite Element Method for Modeling 3D Resistivity Sounding on Anisotropic Geoelectric Media," *Math. Probl. Eng.*, vol. 2017, pp. 1–12, 2017, doi: 10.1155/2017/8027616.
[26] W. Lu, Q. Zhang, and W. Zhou, "Pile Driving Analysis Based on Wave Equation Theory and Finite Element Method," *Journal of Civil Engineering*, vol. 23, no. 4, pp. 56–68, 2020.
[27] L. Sledziewski, L. Sledziewski, and M. Kowalczyk, "Fatigue stresses assessment in welded connections of steel bridge using finite element method," *J. Constr. Steel Res.*, vol. 140, pp. 105–115, 2018.
[28] L. Meng, *Discrete and continuum modeling of brittle and ductile fracture within the framework of finite element method*. search.proquest.com, 2023. [Online]. Available: https://search.proquest.com/openview/fea1162bdc281115efab34cb65d4de2a/1?pq-origsite=gscholar&cbl=18750&diss=y
[29] A. W. Efendi, "Modeling of soil subsidence in IKN using numerical analysis of the finite element method LISA V. 8," *researchgate.net*, 2020, [Online]. Available: https://www.researchgate.net/profile/Aco-Efendi/publication/367090313_Modeling_of_soil_subsidence_in_IKN_using_numerical_analysis_of_the_finite_element_method_LISA_V8/links/63c0f9964c7e7c4e5125262a/Modeling-of-soil-subsidence-in-IKN-using-numerical-analysis-of-the-finite-element-method-LISA-V8.pdf
[30] Badan Standardisasi Nasional, "SNI 7973:2013: Spesifikasi desain untuk konstruksi kayu," 2013, *BSN*.
[31] M. A. Ritter, *Timber construction manual*. John Wiley & Sons, 1990.
[32] R. Gupta, S. Bhatnagar, and S. Khanduja, "Elastic constants of teak wood: A review," *Journal of the Indian Academy of Wood Science*, vol. 1, no. 1, pp. 1–6, 2004.
[33] R. Kumar, S. Agarwal, and D. Sharma, "Mechanical properties of teak wood: A review," *J. For. Res. (Harbin).*, vol. 29, no. 3, pp. 753–761, 2018.
[34] K. J. Bathe, *Finite Element Procedures*. Prentice Hall, 1996.
[35] K. J. Bathe, *Finite Element Procedures*. Upper Saddle River, NJ: Prentice Hall, 2014.
[36] O. J. ACHOLA, *MATHEMATICAL MODELLING OF VARIABLE VISCOSITY HYDROMAGNETIC BOUNDARY LAYER FLOW WITH THERMAL RADIATION AND NEWTONIAN …*. ir-library.ku.ac.ke, 2018. [Online]. Available: https://ir-

library.ku.ac.ke/bitstream/handle/123456789/18847/Mathematical%20Modelling%20of%20Variable%20Viscosity....pdf?sequence=1

[37] B. R. Banting and W. W. El-Dakhakhni, "Force-and displacement-based seismic performance parameters for reinforced masonry structural walls with boundary elements," *Journal of Structural Engineering*, 2012, [Online]. Available: https://ascelibrary.org/doi/abs/10.1061/(asce)st.1943-541x.0000572

[38] R. Purba and M. Bruneau, "Case study on the impact of horizontal boundary elements design on seismic behavior of steel plate shear walls," *Journal of Structural Engineering*, 2012, [Online]. Available: https://ascelibrary.org/doi/abs/10.1061/(ASCE)ST.1943-541X.0000490

[39] Y. Xiao and L. Y. She, *FRP-strengthened timber structures*. Woodhead Publishing, 2019.